Pergamon

Tetrahedron Vol. 50, No. 29, pp. 8579-8596, 1994

0040-4020/94 $7.00+0.00

0040-4020(94)00481-1

SYNTHESIS AND UNUSUAL PROPERTIES OF EXPANDED BILIRUBIN ANALOGS

Daniel F. Nogales, D. Timothy Anstine and David A. Lightner*

Department of Chemistry, University of Nevada
Reno, Nevada 89557-0020 USA

Abstract. **Pentapyrrole analogs of bilirubin and biliverdin have been prepared along with corresponding analogs where two dipyrrinones are attached to *p*-xylyl and *m*-xylyl groups. As determined by spectroscopic analysis and molecular modelling, the "expanded" yellow bilirubin analogs are able to adopt intramolecularly hydrogen bonded conformations.**

INTRODUCTION

Bilirubin is the lipophilic and water insoluble, yellow-orange and neurotoxic pigment of jaundice that is biosynthesized at the rate of ~300 mg/day by heme degradation in healthy adults and excreted across the liver into bile as water-soluble conjugates.[1,2,3] Its constitutional structure is comprised of two dipyrrinones conjoined at their α-carbons to a -CH_2- group.[4] Propeller-like rotations of the dipyrrinones about the -CH_2- create a wide variety of conformations with very different shapes.[5] Of these, the most stable is shaped like a ridge-tile (Fig. 1A) that brings the propionic acid carboxyls and dipyrrinone polar groups into close proximity, into a unique orientation suitable for intramolecular hydrogen bonding.[6] Bilirubin is known to adopt an intramolecularly hydrogen-bonded ridge-tile conformation (Fig. 1A) in crystals[7] and in non-polar solvents.[6,8] But its conformation is less certain in polar organic solvents,[7,8] in lipids,[9,10] in aqueous solution when bound to proteins,[11,12] or in aqueous or organic solvents when the propionic acid groups are ionized to propionate.[13,14,15] It is clear, however, that intramolecular hydrogen bonding can be a dominating factor in pigment hepatic metabolism.[16] Therefore, the ability of bilirubin to fold into a shape ideally suited for intramolecular hydrogen bonding or, alternatively, to rotate its dipyrrinones to generate elongated or compact bilirubin conformers while disengaging hydrogen bonds is a fundamental consideration in the relationship

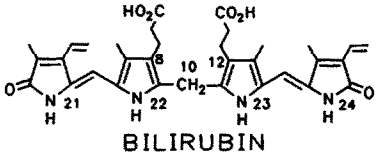

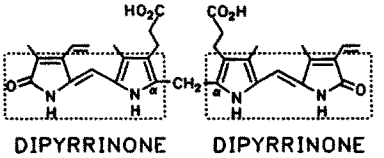

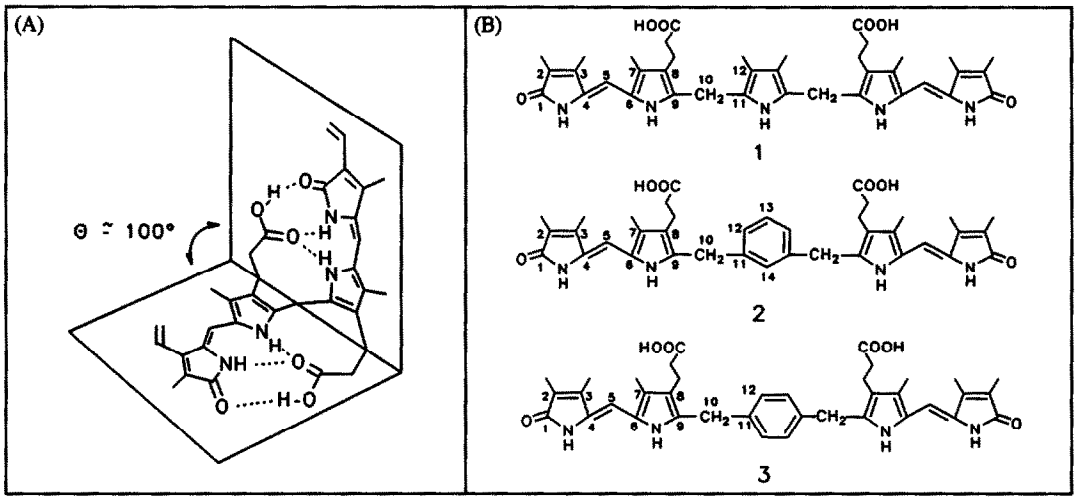

FIGURE 1. (A) Intramolecularly hydrogen-bonded conformation of bilirubin shaped like a ridge-tile or open book. The dihedral fold angle (θ) is ~100°. (B) Expanded bilirubin analogs.

between pigment conformation and amphiphilicity and in the many steps associated with bilirubin transport to the liver, uptake, conjugation and excretion.[3,4,17]

Taken collectively, three structural components appear to control the shape of bilirubin: (i) two dipyrrinone chromophores, each in a *syn*-periplanar conformation with Z-configuration C=C bonds at C_4 and C_{15}; (ii) an sp^3 carbon at C_{10}, which causes the molecule to bend in the middle and allows the two dipyrrinone chromophores to rotate independently about the C_9-C_{10} and C_{10}-C_{11} single bonds; and (iii) two propionic acid groups, located at C_8 and C_{12}, which can form intramolecular hydrogen bonds with the dipyrrinone pyrrole and lactam functions in the opposite half of the molecule (Fig. 1A). Sequestration of the carboxylic acids through intramolecular hydrogen bonding lowers their acidity and increases the lipophilicity of the pigment, rendering it unexcretable in normal metabolism, except by glucuronidation. Structural modifications which do not interfere with structural components (i), (ii) and (iii), as in glaucorubin, afford bilirubin analogs with similar solubility properties. But structural modifications that relocate the propionic acid groups away from C_8 and C_{12}, as in mesobilirubin-IVα, or bridge N_{21} and N_{24} by a -CH_2- are known to have very different solubility properties because intramolecular hydrogen bonding is disengaged.[18,19] Modifications at the C_{10} -CH_2- are largely unknown, except for *gem*-dimethyl substitution;[20] yet, major perturbations at the center of the pigment can be expected to exert a large influence on its conformation and hence its properties. In the following we describe syntheses of three such bilirubin analogs (**1**, **2** and **3** of Synthetic Scheme 1), where

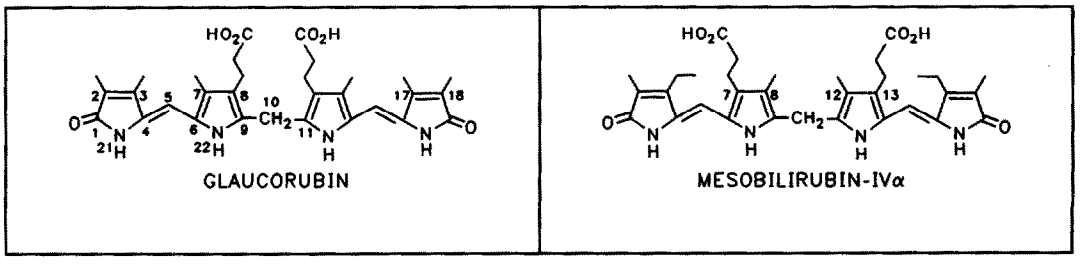

pyrrole and phenyl groups are inserted centrally; analyze their most stable conformations and the role of hydrogen bonding by molecular dynamics computations and by NMR spectroscopy; and compare their properties to bilirubin and glaucorubin.[20]

SYNTHESIS

Our approach to the syntheses of **1**, **2** and **3** involved acid-catalyzed coupling of two equivalents of a suitable α-free dipyrrinone (**10**) with specific pyrrole[21] and benzene dialdehydes, as shown in Scheme 1. The reactions proceeded in two steps in CF_3COOH solvent at 70° during one hour to afford high yields of "verdin"-like condensation products **7** (blue-green), **8** (orange) and **9** (red-brown). Reactions run at room temperature showed no product formation after 18 hours, but at elevated temperatures (70°C) product formation was observed in minutes, and the reactions were usually complete in 1 hour. The reactions were

SYNTHETIC SCHEME 1

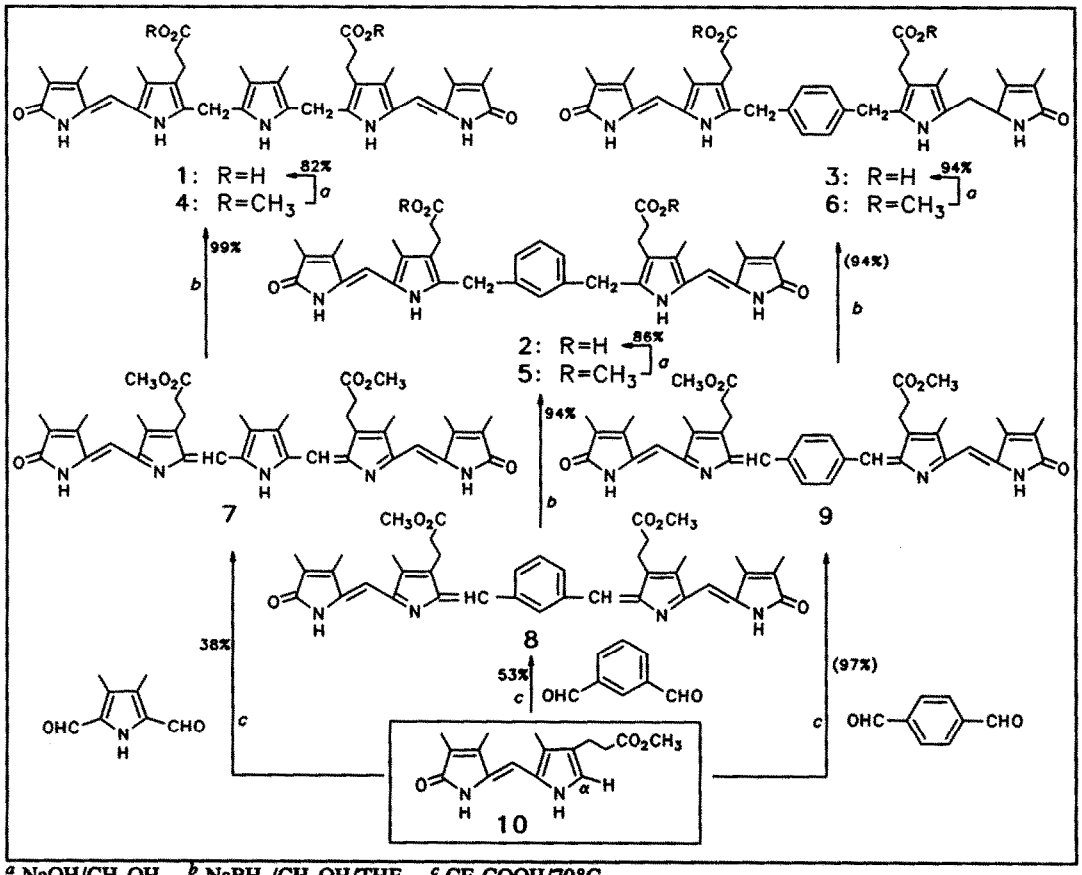

[a] $NaOH/CH_3OH$. [b] $NaBH_4/CH_3OH/THF$. [c] $CF_3COOH/70°C$.

monitored by periodically quenching an aliquot of the reaction mixture with triethylamine and following the disappearance of **10** and the appearance of product by thin layer chromatography. Many attempts using different reaction conditions were made with *o*-phthalaldehyde to synthesis the *ortho* analog of **8** and **9**, but no product formation was detected. Steric hindrance presumably retards this reaction.

The three verdin analogs (**7**, **8** and **9**) could be reduced easily to their corresponding rubin dimethyl esters **4**, **5** and **6** using sodium borohydride in methanol[21b] while sonicating the reaction mixture. Reduction of *para*-isomer **9** proceeded quickly (about 1 hour) to afford **6**, which was only slightly soluble in dimethylsulfoxide but insoluble in dichloromethane and chloroform. The solubility properties are very different from those of bilirubin dimethyl ester, which is soluble in chloroform and in dimethylsulfoxide. The *meta* "verdin" analog (**8**) was also easily reduced to its corresponding rubin dimethyl ester (**5**) in a similarly short reaction time. Unlike the *para*-xylyl rubin dimethyl ester (**6**), the *meta* (**5**) was easily soluble in dichloromethane and exhibited solubility properties similar to those of bilirubin dimethyl ester. Pentapyrrole verdin **7** reacted with sodium borohydride much more sluggishly, with the color remaining blue-green, then gradually turning to red during 3 hours, and finally to yellow (after further addition of sodium borohydride) during one hour. Like **5**, rubin diester **4** was soluble in dichloromethane and dimethylsulfoxide. The target rubin acids (**1**, **2** and **3**) were obtained by saponification of the corresponding rubin esters with sodium hydroxide in methanol-tetrahydrofuran at reflux for 3 hours. The *p*-xylyl rubin ester (**6**) was resistant to saponfication under these conditions, but was successfully converted to **3** by refluxing in ethanolic sodium hydroxide during 18 hours.

The key component dipyrrinone in the reactions of Scheme 1, methyl nor-neoxanthobilinate (**10**) was prepared in gram quantities from simpler monopyrroles, as indicated in Scheme 2. The left half of **10** was synthesized, by modification of known methods.[20] Pyrrole ester **15** was saponified then easily decarboxylated to afford 3,4-dimethylpyrrole (**14**) by distilling at reduced pressure. An alternative to the reported decarboxylative distillation of the acid of **15** is to make a slurry with diethylene glycol and heat the slurry to just below the boiling point of the glycol at aspirator vacuum. Pyrrole **14** distills as a clear, low melting solid in higher yield than that reported for decarboxylation by heating the solid.[20] Pyrrole **14**, which also is a key intermediate in the preparation of dialdehyde **23**, was converted to 3,4-dimethyl-3-pyrrolin-2-one (**12**) in 95% yield by oxidation with hydrogen peroxide.

The right half of dipyrrinone **10** was first synthesized by Woodward *et al.*[22] in the total synthesis of chlorophyll. Starting from 2-carboethoxy-3,5-dimethyl-4-propyl(3-carboethoxy)-1*H*-pyrrole **20**, the α-methyl was perchlorinated using sulfuryl chloride then hydrolyzed to the α-carboxylic acid in high yield (90%) and saponified to give tri-acid **19**. Selective esterification of the propionic acid group (to give **18**) prior to decarboxylation of the α-acid groups led to higher yields and a simplified reaction as compared with that reported.[22] Smooth decarboxylation of diacid-monoester **18**, in a kugelrohr oven, gave light brown opsopyrrole ethyl ester (**16**). Vilsmeier mono-formation of **16**, carried out in dry ether with *N*,*N*-dimethylformamide and $POCl_3$ at 0°C, gave a mixture of two isomeric aldehyde products after hydrolysis: the desired 5-formylpyrrole (**13**) and its isomeric 2-formylpyrrole (**17**) in a ratio of 4:1. The minor isomer could be washed away from the major product using methanol. Isomer **17** is less polar than **13**, possibly due to intramolecular hydrogen bonding between the 2-formyl group and 3-propionic acid group.

Coupling 3-pyrrolin-2-one **12** with 5-formyl pyrrole **13** was achieved in methanol-aqueous potassium hydroxide overnight at room temperature. After acidification, the desired nor-neoxanthobilirubic acid (**11**) was isolated by filtration in a high yield (90%) and in gram quantities. Conversion of **11** to its methyl ester

10 was accomplished with diazomethane in methanol to give the key starting material for preparing the expanded bilirubin analogs as outlined in Scheme 1.

SYNTHETIC SCHEME 2

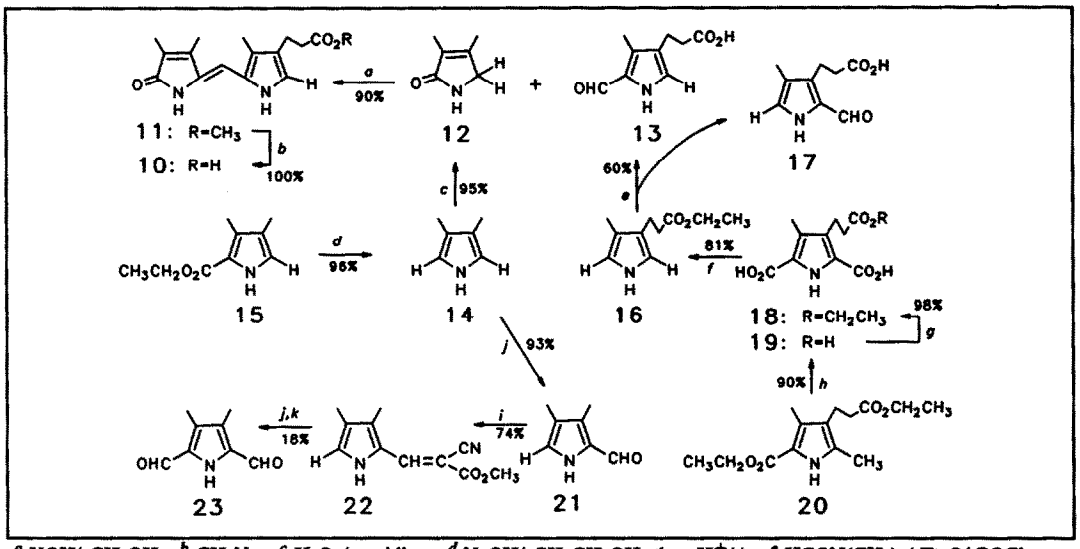

[a] KOH/ CH_3OH. [b] CH_2N_2. [c] H_2O_2/ pyridine. [d] NaOH/ CH_3CH_2OH, then H^+/Δ. [e] $HCON(CH_3)_2$/ Et_2O/ $POCl_3$, then evap./ NaOH/H_2O, Δ. [f] Δ, distil. [g] $HC(OCH_2CH_3)_3$/ CF_3CO_2H. [h] SO_2Cl_2, then NaOH. [i] $CH_2(CN)CO_2CH_3$/ $(CH_3CH_2)_2NH$ cat. [j] $HCON(CH_3)_2$/ $ClCH_2CH_2Cl$-$POCl_3$, reflux, then NaOAc/H_2O, reflux. [k] KOH/ CH_3OH, reflux.

Terephthalaldehyde and isophthaldehyde are commercially available, and 2,5-diformyl-3,4-dimethyl-1*H*-pyrrole (**23**) was synthesized from 3,5-dimethylpyrrole (**14**). Vilsmeier formylation reaction of **14** gave the mono-aldehyde **21**. Attempts to diformylate **14** in one step failed using a variety of harsh reaction conditions. So, attachment of the second formyl group was accomplished in three steps from **21** by protecting the formyl group as its condensation product with methyl cyanoacetate to give **22**.[23] followed by a second Vilsmeier reaction carried out in high yield (81%), using conditions described previously.[24] Deprotection with potassium hydroxide followed by thorough extraction with dichloromethane gave the desired diformylpyrrole (**23**) in 22% yield.

RESULTS AND DISCUSSION

Rubin Acids. The assigned constitutional structures of the expanded bilirubin analogs (**1-3** of Fig. 1) are consistent with their ^{13}C-NMR spectral data (Table 1), which show signals that correlate well with the expected molecular symmetry. The ^{13}C chemical shifts of the component dipyrrinones compare very favorably with those of glaucorubin (the symmetric analog of bilirubin with vinyl groups are replaced by methyls), suggesting no strong perturbing interactions between the central xylyl or pyrrolyl units and the flanking dipyrrinones. The carbon signals from the central units are easily distinguished and are fully consistent with expectations: a 3,4-dimethyl-2,5-methylenopyrrolyl unit in **1**, a *m*-xylyl in **2** and a *p*-xylyl in **3**.

Table 1. Comparison of ^{13}C-NMR Chemical Shifts and Assignments of Expanded Bilirubin Analogs 1-3 with Glaucorubin (G) in $(CD_3)_2SO$[a]

Position[b]	Carbon	1	2	3	G
1	C=O	172.05	171.9	172.4	172.0
2	=C—	122.6	122.3	122.8	122.5
2^1	CH_3	8.98	9.18	9.70	8.10
3	=C—	141.5	141.5	142.0	147.2
3^1	CH_3	8.23	8.34	8.80	9.40
4	=C—	131.9	131.6	132.4	130.4
5	=CH—	98.06	97.70	98.17	97.80
6	=C—	121.9	122.3	122.7	122.0
7	=C—	122.8	123.6	124.1	122.9
7^1	CH_3	9.58	9.58	10.04	9.25
8	=C—	118.8	119.4	119.7	119.2
8^1	CH_2	19.31	19.48	19.85	19.27
8^2	CH_2	34.66	34.88	34.38	35.34
8^3	C=O	174.2	174.1	174.5	174.0
8^4	OCH_3	—	—	—	—
9	=C—	128.9	129.0	129.5	128.8
10	$-CH_2-$	22.45	31.21	31.35	23.55
11	=C—	123.5	140.3	138.2	—
12	=C-/=CH-	112.2	125.6	128.4	—
13/14	=CH—	—	127.6/ 128.4	—	—
12^1	CH_3	9.12	—	—	—

[a] Run at 2.5×10^{-2} M concentration of pigment at 22°C with chemical shifts recorded in ppm downfield from $(CH_3)_4Si$. Multiplicities are determined by the APT method. [b] Superscripts refer to carbons in the β-substituent chains, e.g. 2^1 is the first carbon attached to ring carbon C_2, and 8^2 is the propionic acid α-carbon.

The expanded bilirubin analogs (1-3) all have similar solubility properties. They exhibit very limited solubility in most organic solvents and are most soluble in dimethylsulfoxide. This behavior is even more exaggerated than the minor solubility differences between bilirubin and glaucorubin and indicates that 1-3 are more polar than either. The low solubility of 1-3 in chloroform made it impossible to determine their ^{1}H-NMR spectrum in $CDCl_3$, although spectra could be obtained in $(CD_3)_2SO$ (Table 2). Although ^{1}H-NMR has been used to detect intramolecular hydrogen bonding in bilirubins[7,25] (for example, compare the ^{1}H-NMR N*H* and COO*H* signals in $CDCl_3$ and in $(CD_3)_2SO$ of glaucorubin (G)); unfortunately it has not yet been possible to use this technique to detect hydrogen bonding in 1-3 where it might be most expected. However, other evidence suggests that intramolecular hydrogen bonding might be important in 1-3.

TABLE 2. Comparison of ^{1}H-NMR Chemical Shifts, Multiplicities[a] and Assignments of Expanded Bilirubin Analogs **1-3** with Glaucobilin (G) in $(CD_3)_2SO$.[b]

Position	Proton	1	2	3	G	G[c]
8^3	CO_2H	11.70	11.95	11.99	11.89	13.59
21	NH	9.66	9.71	9.76	9.78	10.61
22	NH	10.22	10.31	10.32	10.32	9.15
5	=CH—	5.87	5.87	5.89	5.94	6.04
10	CH_2	3.71	3.84	3.84	3.95	4.07
23	NH	9.15	—	—	—	—
8^1	CH_2	2.45[d]	2.46[d]	2.50[d]	2.41[e]	2.50-3.00
8^2	CH_2	2.05[e]	2.09[e]	2.14[e]	1.92[e]	2.50-3.00
7^1	CH_3	1.96	2.01	2.01	2.05	2.16
3^1	CH_3	1.68	1.72	1.72	2.00	2.06
12^1	CH_3	2.00	—	—	—	—
2^1,18^1	CH_3	1.79	1.97	1.99	1.77	1.85
12	=CH—	—	6.91	7.04	—	—
13/14	=CH—	—	7.15/6.94	—	—	—

[a] Singlets, unless otherwise noted. [b] Run at 10^{-3} *M* concentration at 22°C with chemical shifts recorded in ppm downfield from $(CH_3)_4Si$. [c] In $CDCl_3$. [d] Signal under d_5-$(CHD_2)CD_3SO$. [e] J=7.5 Hz. [f] Lies under 12^1 CH_3.

The greater polarity of **1**, **2** or **3** as compared with bilirubin is revealed by their reverse phase HPLC retention times. Using McDonagh's buffer[26] (0.1 *M* di-*n*-octylamine acetate, in methanol, pH 7.7, 5% H_2O) as eluent and bilirubin as a reference standard (retention time 16 minutes), glaucorubin elutes faster (11.2 minutes) and **1** is comparably fast (11.5 minutes), but **2** and **3** elute even faster (8 and 7 minutes, respectively). These data suggest that **1** may be intramolecularly hydrogen bonded somewhat comparably to glaucorubin (as in Fig. 1A) and that **2** and **3** are less well intramolecularly hydrogen bonded. The HPLC method is very sensitive to small changes, however. For example, mesobilirubin-XIIIα and glaucorubin differ only in that the former has ethyl groups in place of methyl at C_3 and C_{17}, but the latter elutes ~5 minutes faster than the former. Thus, the differing retention times between **1** and **2** or **3** may also reflect the change of the central ring from pyrrole to phenyl.

Although their limited solubility in organic solvents has so far thwarted efforts to use ^{1}H-NMR as a probe of conformation of the expanded bilirubin analogs **1-3** in $CDCl_3$ solvent, they are sufficiently soluble for UV-visible spectral determinations (Table 3). The relatively invariant λ_{max} over a range of solvent polarity for the *p*-xylyl expanded bilirubin (**3**) fits a picture where the conformation is relatively invariant, possibly an extended conformation similar to that drawn in Fig. 1B, with little or no intramolecular hydrogen bonding. In contrast, the *m*-xylyl analog (**2**) exhibits shifts in λ^{max} values, with a shorter wavelength λ^{max} absorption found in the less polar solvent. That is, unlike the *p*-xylyl analog, the UV-visible band of the *m*-xylyl analog is blue-shifted in non-polar solvents and shifted to the red in polar solvents. In dimethylsulfox-

ide, for example, the UV-visible band of **2** and **3** are nearly identical. The data suggest a more folded conformation for **2** in non-polar solvents, probably stabilized by intramolecular hydrogen bonds — and a more stretched conformation in polar solvents where intramolecular hydrogen bonds are broken.

TABLE 3. Comparison of UV-visible Long Wavelength Absorption of Expanded Bilirubin Analogs **1-3**.

Solvent	Pentapyrrole rubin		*m*-xylyl rubin **2**		*p*-xylyl rubin **3**		Glaucorubin		Dipyrrinone **11**	
	λ^{max} (nm)	ϵ (M^{-1} cm^{-1})	λ^{max} (nm)	ϵ (M^{-1} cm^{-1})	λ^{max} (nm)	ϵ (M^{-1} cm^{-1})	λ^{max} (nm)	ϵ (M^{-1} cm^{-1})	λ^{max} (nm)	ϵ (M^{-1} cm^{-1})
Benzene	390	63,000	402	45,100	410	43,200	433	54,300	391	31,600
$CHCl_3$	404	44,100	414	51,700	409	50,600	431	58,000	397	26,500
CH_3OH	383	62,000	397	54,400	409	54,100	insol	insol	395	27,000
$(CH_3)_2NCHO$	412	55,500	408	51,300	403	46,700	419	50,600	392	30,000
$(CH_3)_2SO$	409	52,070	405	46,900	405	43,400	426	57,300	395	30,000

In the pentapyrrole analog **1**, the UV-visible spectra are solvent dependent — qualitatively like those of **2** — with the blue-shifted spectra in non-polar solvents and red-shifted spectra in polar solvents. As in **2** the data suggest a conformational change from a more folded (and probably intramolecularly hydrogen-bonded) conformation in non-polar solvents to a more open shape (probably without intramolecular hydrogen bonds) in polar solvents. The data in methanol remain an exception, as **1** appears to prefer a more folded conformation; whereas, **2** adopts a more open conformation. Taken collectively, the UV-visible data implicate the role of much stronger intramolecular hydrogen bonds in **1** than in **2**.

These data are important because bilirubins are bichromophoric molecules, and the relative orientation of the two dipyrrinone chromophores determines the shape and λ^{max} of the pigment's long wavelength absorption band. UV-visible and circular dichroism spectra are characteristic of two coupled chromophores with little orbital overlap between them and strongly allowed long wavelength transitions. In the case of the ridge-tile conformation of bilirubin ($\epsilon_{420} \sim 35{,}000$) (Fig. 1A) maximum exciton interaction between the component dipyrrinone intense long wavelength electronic transitions obtains for a folded conformation, where minimum interchromophoric orbital interaction (homoconjugation) results.[5,6] However, as the relative orientation of the dipyrrinone chromophores shifts toward the linear conformations (as θ of Fig. 1A increases) or the porphyrin-like (*e.g.*, as θ of Fig. 1A decreases), the spectrum shifts. The porphyrin-like, the ridge-tile and the linear conformations of bilirubins correspond to the classical cases for parallel, oblique and linear orientations of the induced electric dipole transition moments studied in detail by Kasha *et al.*[27] (Fig. 2). In the ridge-tile conformation (Fig. 1A), both exciton transitions are allowed and may be seen, *e.g.*, in glaucorubin's long wavelength UV-visible spectrum as a broad band centered near 430 nm in chloroform (Table 3). As the pigment unfolds toward the linear shape ($\theta \rightarrow 180°$), the UV-visible band is expected to sharpen and red-shift as the transition probability to the lower energy exciton state increases. As the pigment folds more toward a porphyrin shape ($\theta \rightarrow 0°$), the long wavelength UV-visible band is expected to sharpen and blue-shift as the transition probability to the higher energy exciton state increases.

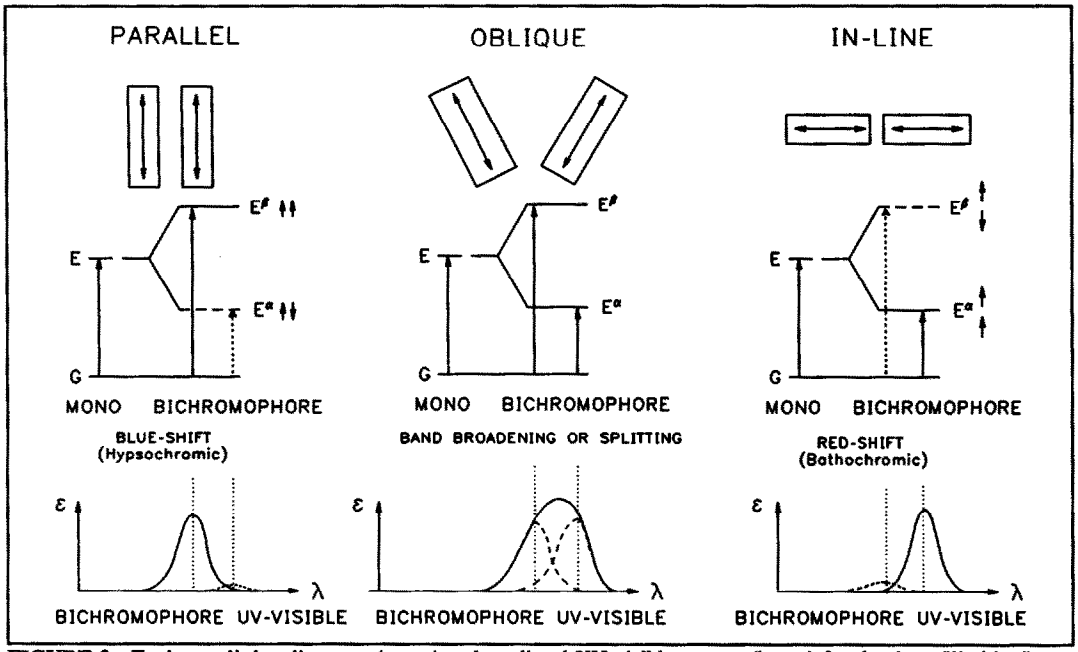

FIGURE 2. Exciton splitting diagrams (upper) and predicted UV-visible spectra (lower) for the three "limiting" case geometrical arrangements of the electric transition moments: parallel, oblique (of which there are many possible), and linear. The parallel case is represented approximately by the porphyrin-like conformation and the in-line, very approximately by the linear conformation of bilirubin. The oblique case is found in a vast array of folded or helical conformations most notably in the ridge-tile conformation (Fig. 1A). The consequences of the three differing alignments of the electric transition dipoles in the bichromophore may be seen in the differing UV-visible spectra.

Molecular Dynamics Calculations. Further insight into the preferred conformation(s) and the importance of intramolecular hydrogen bonding can be obtained from molecular dynamics computations.[5] A multitude of conformations in **1**, **2** and **3** are possible by independent rotations about the two -CH_2- groups connecting two dipyrrinones to a central aromatic ring. Molecular modelling predicts considerable conformational stabilization following rotation of the dipyrrinones into a position for intramolecular hydrogen bonding with the opposing propionic acid residues — similar to that seen in bilirubin (Fig. 1A).[5-8] The global energy minimum conformations are shown in ball and stick format in Fig. 3. In these conformations the dipyrrinones are rotated into nearly parallel planes, forming sandwich-like shapes. Intramolecular hydrogen bonding causes the dipyrrinones to tilt toward one another at their extrema by pulling the opposing lactam groups toward each other. In **3**, only partial hydrogen bonding is possible, as the top part (Fig. 3C, right) of the molecule is more extended than in **1** and **2**. This means that the sandwich conformation is rendered relatively less stable in **3** than in **1** or **2**. Comparison of the computed ΔH_f values for **2** and **3** predict that **2** will be some 18 kcal/mole more stable than **3**. These data suggest that stabilization of the sandwich-shape global minimum conformation of **3** is only slight. Consequently, even in solutions where solvents do not interfere with intramolecular hydrogen bonding, **3** probably exhibits no special stabilization of the sandwich conformation, but **1** and **2** probably do. These cup-like conformations may be suitable for enclosing guest molecules in molecular recognition studies.

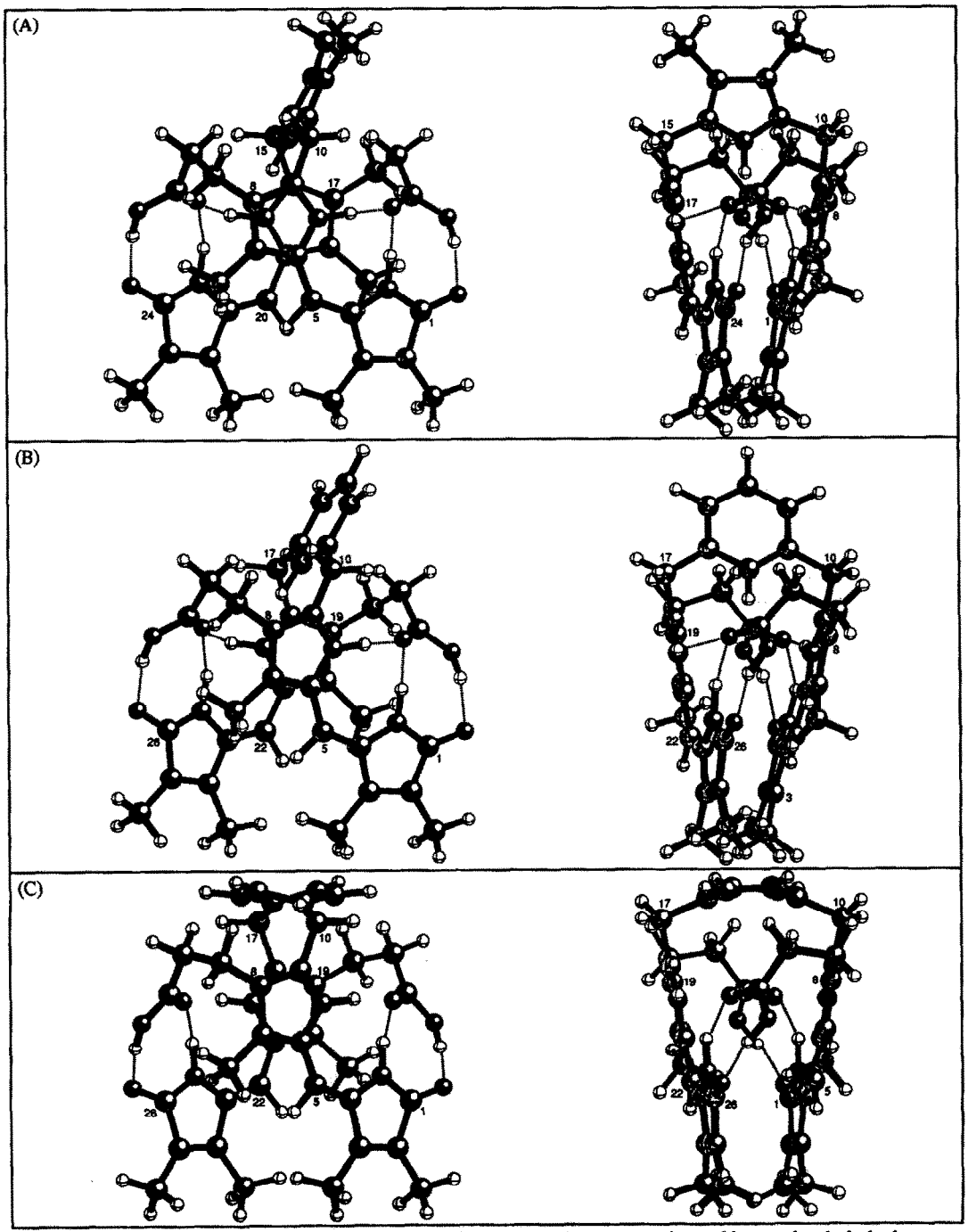

FIGURE 3. (Left) Top view and (Right) side view of ball and stick representations of intramolecularly hydrogen-bonded global energy minimum conformations of (A) pentapyrrole rubin **1**, (B) *m*-xylyl rubin **2** and (C) *p*-xylyl rubins **3**. Intramolecular hydrogen bonds are shown in dashed lines.

Rubin Esters. Information on the conformation of the expanded rubin dimethyl esters may be extracted from their ^{1}H-NMR and UV-visible spectra. The N-*H* chemical shifts of **4-6** in $(CD_3)_2SO$ are all very similar to the corresponding lactam and pyrrole N-*H* chemical shifts of glaucorubin dimethyl ester (Table 4), indicating that the dipyrrinones are hydrogen bonded to solvent, as expected from other studies.[24] In $CDCl_3$, glaucorubin dimethyl ester is thought to exist as an intermolecularly hydrogen bonded dimer, and its lactam N-*H* becomes slightly more deshielded than the pyrrole N-*H*. In **4** and **5** (**6** is insoluble in $CDCl_3$), the lactam and pyrrole N-*H* signals are even more strongly deshielded than in glaucorubin dimethyl ester — as if intramolecular hydrogen bonding had intensified.

TABLE 4. Comparison of N-*H* Chemical Shifts of Expanded Bilirubin Dimethyl Esters (**4-6**) with Glaucobilin Dimethyl Ester (**GE**) in $CDCl_3$ and $(CD_3)_2SO$.

Compound	Chemical Shift in $CDCl_3$		Chemical Shift in d_6-DMSO	
	Lactam N-*H*	Pyrrole N-*H*	Lactam N-*H*	Pyrrole N-*H*
Pentapyrrole dimethyl ester **4**	10.96	10.40	9.64	10.13
m-Xylylrubin dimethyl ester **5**	11.35	10.72	9.69	10.31
p-Xylylrubin dimethyl ester **6**	not soluble	not soluble	9.75	10.33
Glaucobilin dimethyl ester (**GE**)	10.44	10.28	9.78	10.41

Further insight into the conformation of esters **4** and **5** may be gained from an examination of -CH_2- splittings (Table 5). The C_{10} -CH_2- of **GE** is a singlet, but in **4** and **5** the hydrogens are non-equivalent, and a large geminal splitting is observed. In addition, the -CH_2-CH_2- propionic ester segment of **4** and **5** is apparently much less flexible than in GE and shows well-defined doublets of doublets of doublets in **4** and doublets of triplets in **5** — in contrast to the simple triplet in GE. The splittings in the propionic segment are more like those seen in bilirubin (ddd for ABCX) than its esters (t for A_2B_2) and are consistent with a picture where motion in the propionic acid groups of **4** and **5** is restricted by *intra*molecular hydrogen bonding (Fig. 3).

TABLE 5. Comparison of the Propionic Ester -CH_2-CH_2- Segment and C_{10} -CH_2- ^{1}H-NMR Splittings in Expanded Rubin Dimethyl Esters **4** and **5** with Those of Glaucorubin Dimethyl Ester (GE) in $CDCl_3$.[a]

Partial Structure	CH_2	**4**	**5**	**GE**
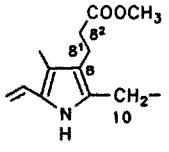	8^1	2.73 (2H, ddd)[b,c,d] 2.65 (2H, ddd)[b,f,g]	2.66 (4H, t, J=8.2Hz)[e]	2.52 (4H, t, J=7.5 Hz)
	8^2	2.22 (2H, ddd)[c,f,h] 2.10 (2H, ddd)[d,g,h]	1.75 (2H, dt, J=16, 8.2 Hz) 2.15 (2H, dt, J=16, 8.2 Hz)	2.25 (4H, t, J=7.5 Hz)
	10	3.70 (2H, d, J=16 Hz) 3.89 (2H, d, J=16 Hz)	3.80 (2H, d, J=14.5Hz) 4.25 (2H, d, J=14.5Hz)	3.83 (2H, s)

[a] Chemical shifts in δ, ppm downfield from $(CH_3)_4Si$. [b] J_{AB}=11.1 Hz. [c] J_{AC}=8.5 Hz. [d] J_{AD}=6.1 Hz. [e] The triplet at 2.66 pm in **5** should be a dt, but the two hydrogens at 8^1 have identical chemical shifts. [f] J_{BC}=5.6 Hz. [g] J_{BD}=9.2 Hz. [h] J_{CD}=13.8 Hz.

Verdin Esters. As seen visually, "verdin" esters are bright red (**9**), yellow-orange (**8**) and green (**7**). More effective conjugation through the *p*-xylylene of **9** in contrast with the *m*-xylylene of **8** is apparently responsible for the color difference. This can also be seen in the relative positions of the long wavelength absorption bands of **8** and **9** (Table 6). Unlike the phenyl analogs, the pentapyrrole verdin **7** has a weak band near 725 nm. This "blue" band plus the more intense "yellow" band near 460 nm gives **7** its green color.

TABLE 6. Comparison of UV-Visible Spectral Data for Expanded Verdin Dimethyl Esters **7-9**.

Solvent	Pentapyrrole-verdin dimethyl ester **7**		*m*-Xylyl-verdin dimethyl ester **8**		*p*-Xylyl-verdin dimethyl ester **9**	
	λ^{max}(nm)	ϵ (M^{-1} cm^{-1})	λ^{max}(nm)	ϵ (M^{-1} cm^{-1})	λ^{max}(nm)	ϵ (M^{-1} cm^{-1})
$CHCl_3$	328	57,000	287	59,200	310	58,600
	459	21,300	455	33,300	523	40,000
	729	8,900	—	—	557(sh)	32,500 (sh)
CH_3OH	321	59,500	279	59,200	309	57,800
	456	21,000	409	30,300	512	35,000
	726	9,800	—	—	544 (sh)	29,000 (sh)
$(CH_3)_2SO$	327	58,900	283	66,600	310	47,400
	454	24,200	435	31,300	525	32,000
	722	9,600	—	—	560 (sh)	26,400 (sh)

CONCLUDING COMMENTS

The dipyrrinone units in the pentapyrrole and in the *m*-xylyl analogs (**1** and **2**) are able to form intramolecular hydrogen bonds with their propionic acid groups, stabilizing sandwich-like conformations. The more elongated *p*-xylyl analog (**3**) is also able to form an intramolecularly hydrogen bonded conformation, but the hydrogen bonds are longer and weaker, and the sandwich conformation is probably relatively less stable. Analog **3** is considerably more polar than **1** and **2** on reverse-phase HPLC, and it is less soluble in organic solvents — all characteristics of a relatively more polar compound as compared with **1** and **2**.

EXPERIMENTAL

General Procedures. All ultraviolet-visible spectra were recorded on a Perkin-Elmer 3840 diode array or Cary 219 Nuclear magnetic resonance (NMR) spectra were determined on a GE QE-300 300-MHz or Varian Unity 500 MHz spectrometer and reported in δ ppm downfield from $(CH_3)_4Si$. Melting points were determined on a Thomas-Hoover capillary apparatus and are uncorrected. Mass spectral data were obtained on a Hewlett Packard 5970 mass selective detector unless otherwise stated. High resolution mass spectra were determined by Midwest Center for Mass Spectrometry, Lincoln, Nebraska. Combustion analyses were determined by Desert Analytics, Tucson, AZ. Analytical thin layer chromatography was carried out on J.T. Baker silica gel IB-F plates (125 μ layers). Flash column chromatography was carried out using Woelm silica gel F, thin layer chromatography grade. HPLC analyses were carried out on a Perkin-Elmer Series 4 high performance liquid chromatograph with an LC-95 UV-visible spectrophotometric detector (set at 410 nm)

equipped with a Beckman-Altex ultrasphere-IP 5 μm C-18 ODS column (25 x 0.46 cm) and a Beckman ODS precolumn (4.5 x 0.46 cm). The flow rate was 1.0 mL/minute, and the elution solvent was 0.1 *M* di-*n*-octylamine acetate in 5% aqueous methanol (pH 7.7, 31°C).[26]

Spectral data were obtained in spectral grade solvents (Aldrich or Fisher). Isophthaldehyde, terephthaldehyde, 2-butanone, ethyl formate, diethyl malonate, sulfuryl chloride, trifluoroacetic acid, acetic acid, tetrahydrofuran, *N,N*-dimethylformamide, phosphorous oxychloride, acetonitrile, and dimethylsulfoxide were from Aldrich. Tetrahydrofuran was dried by distillation from sodium.

Methyl 3-Nor-neoxanthobilirubinate (10). Excess etheral diazomethane was added to 3-nor-neoxanthobilirubic acid (**11**)[20] (100 mg, 0.36 mmole) suspended in 60 mL of methanol. The mixture was stirred for 1 hour after which the solvent was evaporated to dryness. The residue was dissolved in 5 mL of dichloromethane and passed through a short column of silica gel (Woelm TLC grade F-DC 35/41, 18% water), eluting with dichloromethane. This procedure gave 10.5 mg (100% yield) of very pure methyl ester **11**. It had mp 205-206°C [Lit.[20] mp 195-197°C]; IR (KBr) ν: 3361, 2915, 1728, 1655, 1637, 1400, 1271, 1111, 693 cm^{-1}. UV/vis: ϵ_{388}^{max} = 29,500 ($CHCl_3$); $\Delta\epsilon_{394}^{max}$ = 27,500 (CH_3OH); $\Delta\epsilon_{394}^{max}$ = 31,000 ($(CH_3)_2SO$); ^{1}H-NMR ($CDCl_3$) δ: 1.94 (s, 3H), 2.12 (s, 3H), 2.14 (s, 3H), 2.57 (t, 2H, J=7.2 Hz), 2.78 (t, 2H J=7.2 Hz), 3.68 (s, 3H), 6.12 (s, 1H), 6.82 (s, 1H), 10.30 (brs, NH), 10.87 (brs, NH) ppm; ^{1}H-NMR ($(CD_3)_2SO$) δ: 1.74 (s, 3H), 1.97 (s, 3H), 2.00 (s, 3H), 2.46 (t, 2H, J=7.2 Hz), 2.68 (5, 2H, J=7.2 Hz), 3.55 (s, 3H), 5.92 (s, 1H), 6.76 (s, 1H), 9.66 (s, 1H), 10.48 (s, 1H); ^{13}C-NMR ($CDCl_3$) δ: 8.22 (q), 9.38 (q), 9.36 (q), 20.74 (t), 34.84 (t), 51.57 (q), 101.1 (d), 120.6 (d), 122.7 (s), 123.3 (s), 124.3 (s), 124.4 (s), 128.9 (s), 142.5 (s), 173.7 (s), 174.2 (s) ppm.

2-(2-Cyano-2-(methoxycarbonyl)vinyl)-3,4-dimethyl-1*H*-pyrrole (22). 2-Formyl-3,4-dimethyl-1*H*-pyrrole (**21**)[23] (1.2 g, 9.8 mmoles) and methyl cyanoacetate (1.3 g) were combined in a 50 mL round-bottom flask with methanol (20 mL). Diethylamine (5 drops) was added and the reaction was heated at reflux for 30 minutes. Upon cooling to room temperature, a solid precipitate was obtained and collected by filtration. This procedure yielded the desired protected aldehyde in 74% (1.5 g). It had mp 189-190°C [Lit.[23] 190-191°C]; IR (KBr) ν: 3399, 2957, 2206, 1707, 1599, 1549, 1242, 1109 cm^{-1}; ^{1}H-NMR ($CDCl_3$) δ: 2.04 (s, 3H), 2.18 (s, 3H), 3.70 (s, 3H), 6.98 (d, 1H, J=2 Hz), 8.00 (s, 1H), 9.65 (bs, 1H) ppm; ^{13}C-NMR ($CDCl_3$) δ: 9.98. 10.02, 53.30, 188.3, 119.9, 123.3, 124.3, 128.3, 134.3, 139.6, 166.3 ppm; GC-MS (*m/z*): 204 (M^+), 172, 145, 118, 91, 89, 65 amu.

2-Cyano-2-(methoxycarbonyl)vinyl)-5-formyl-3,4-dimethyl-1*H*-pyrrole. In a 100 mL round-bottom flask, *N,N*-dimethylformamide (0.5 mL) was cooled to 0°C; then phosphorous oxychloride (0.4 mL, 0.6 g) was added slowly over a period of 30 minutes. The solution was warmed to room temperature and stirred for 10 minutes. Dry 1,2-dichloroethane (20 mL) was then added followed by 2-(cyano-2-(methoxycarbonyl)vinyl)-3,4-dimethyl-1*H*-pyrrole (**22**) (0.8 g, 3.7 mmoles). The flask was equipped with a reflux condenser and the mixture was heated at reflux for 15 minutes. The solution was then cooled to room temperature, and sodium acetate · 3 H_2O (10 g in 40 mL of H_2O) was added and heated reflux for an additional 15 minutes, then cooled to room temperature. The reaction was extracted with dichloromethane (2 x 30 mL), dried over magnesium sulfate, and evaporated (roto-vap) to dryness to yield 2-(cyano-2-(methoxycarbonyl)vinyl)-5-formyl-3,4-dimethyl-1*H*-pyrrole (0.7 g, 81%). It had mp 159-162°C [Lit.[23] 168°C]; IR (KBr) ν: 3294, 2927, 2227,

1722, 1674, 1605, 1467, 1260, 1225, 1095, 1016 cm^{-1}; ^{1}H-NMR ($CDCl_3$) δ: 2.15 (s, 3H), 2.30 (s, 3H), 3.90 (s, 3H), 8.05 (s, 1H), 9.85 (s, 1H), 10.1 (bs, 1H) ppm; ^{13}C-NMR ($CDCl_3$) δ: 8.35, 8.89, 62.54, 98.25, 118.3, 128.3, 129.0, 134.3, 139.1, 163.3, 178.7, 179.2 ppm; GC-MS (*m/z*): 232 (M^+), 201, 172, 144, 129, 118, 89, 65 amu.

2,5-Diformyl-3,4-dimethyl-1*H*-pyrrole (23). In a 50 mL round-bottom flask 2-(cyano-2-(methoxycarbonyl)vinyl)-5-formyl-3,4-dimethyl-1*H*-pyrrole (0.7 g, 0.3 mmoles), potassium hydroxide (8 g, in 8 mL of H_2O) and ethanol (8 mL) were combined and heated at reflux for 20 minutes. The solution was chilled and acidified carefully with 6*N* H_2SO_4 to pH 5. The resulting precipitate was dissolved in water (50 mL) and extracted thoroughly with dichloromethane (5 x 30 mL). The organic phase was dried over magnesium sulfate, filtered and evaporated (roto-vap) to dryness. This procedure yielded 100 mg of 2,4-formyl-3,4-dimethyl-1H-pyrrole (22% non-optimized). It had mp 145-149°C [Lit.[23] 158 °C]; IR (KBr) ν: 3170, 1640, 1469, 1400, 1238 cm^{-1}; ^{1}H-NMR ($CDCl_3$) δ: 2.31 (s, 6H), 9.5 (bs, 1H), 9.87 (s, 2H) ppm; ^{13}C-NMR ($CDCl_3$) δ: 8.08, 129.4, 131.6, 179.9 ppm; GC-MS (*m/z*): 151 (M^+), 136, 122, 105, 94, 77, 67, 52 amu.

(4*Z*,9*Z*,15*Z*,20*Z*)-2,3,7,12-13,18,22,23-Octamethyl-(1*H*,24*H*,25*H*,27*H*,29*H*)-pentapyrrin-1,24-dione-8,17-dipropanoic Acid Dimethyl Ester (7). In a 25 mL round-bottom flask methyl 3-nor-neoxanthobilirubinate (**10**) (100 mg, 0.347 mmoles) and 2,5 diformyl-3,4-dimethylpyrrole (**23**) (26 mg, 0.015 mmoles) were combined, and trifluoroacetic acid (15 mL) was added dropwise. The flask was equipped with a reflux condenser, and the solution was stirred magnetically and blanketed with nitrogen. The reaction mixture was heated to 70°C for 2.5 hours in the dark, then cooled to 5°C. Triethyl amine (15 mL) was added slowly to neutralize the reaction, and the solution was taken up in dichloromethane (25 mL), washed with water (3 x 20 mL) and dried over magnesium sulfate. The magnesium sulfate was removed by filtration, and the dichloromethane was removed (roto-vap), to give a green-brown solid. Methanol (5 mL) was added, and the solid was digested for 5 minutes. The mixture was filtered and washed with additional methanol (5 mL) to give the desired product (**7**) as a blue-green solid (40 mg, 38%). The compound was further purified by flash chromatography (TLC silica gel deactivated with 10% water) using dichloromethane/methanol 99:1 as solvent. It had mp 264-265°C; IR (KBr) ν: 3378, 2916, 1736, 1700, 1584, 1393, 1217, 1105, 751 cm^{-1}; UV-vis in Table 6; ^{1}H-NMR ($CDCl_3$) δ: 1.78 (s, 3H), 2.02 (s, 6H), 2.03 (s, 6H), 2.31 (s, 3H), 2.65 (t, 4H, J=8 Hz), 2.95 (t, 4H, J=8 Hz), 3.69 (s, 3H), 5.67 (s, 2H), 6.97 (s, 2H), 8.39 (s, 1H), 11.34 (bs, 2H) ppm; ^{13}C-NMR ($CDCl_3$) δ: 8.50 (q), 9.49 (q), 9.59 (q), 9.78 (q), 20.10 (t), 35.52 (t), 51.70 (d), 96.34 (d), 112.5 (d), 129.5 (s), 129.8 (s), 134.5 (s), 136.7 (s), 139.4 (s), 141.8 (s), 142.7 (s), 153.0 (s), 167.4 (s), 170.3 (s), 173.5 (s) ppm.

Anal. Calcd for $C_{40}H_{45}O_6N_5$ (691.8): C, 69.45; H, 6.56; N, 10.12.
Found: C, 68.99; H, 6.31; N, 10.31.

1,3-Phenyldimethylene-bis-{2-[5-(1.5-didehydro-3,4-dimethyl-5-oxo-2*H*-pyrrole-2-ylidene methyl)-4-methyl-2*H*-pyrrole-3-propanoic Acid Methyl Ester]} (8). Methyl 3-nor-neoxanthobilirubinate (**10**) (100 mg, 0.347 mmoles) and isophthalaldehyde (22 mg, 0.015 mmoles) were condensed exactly as for **7** above. The product was obtained as an orange solid (62 mg, 53%). The compound was further purified by flash chromatography (TLC silica gel deactivated with 10% water) using dichloromethane/methanol 99:1 as solvent. It had mp 250-252°C; UV-vis in Table 6; IR (KBr) ν: 3280, 2975, 1738, 1703, 1615, 1456, 1362, 1271, 1165, 1093, 957, 916, 687 cm^{-1}; ^{1}H-NMR δ: 1.91 (s, 6H), 2.05 (s, 6H), 2.08 (s, 6H), 2.59 (t, 4H, J=7.2

Hz), 3.00 (t, 4H, J=7.2 Hz), 3.67 (s, 6H), 5.77 (s, 6H), 6.97 (s, 2H), 7.57 (t, 1H, J=7.8 Hz), 7.99 (d, 2H, J=7.8 Hz) 9.22 (s, 1H), 10.5 (bs, 2H) ppm: ^{13}C-NMR ($CDCl_3$) δ: 8.64 (q), 9.53 (q), 9.81 (q), 19.91 (t), 35.34 (t), 51.61 (d), 94.85 (d), 128.4 (d), 129.2 (d), 130.8 (s), 133.6 (d), 134.7 (s), 135.7 (d), 136.4 (s), 139.9 (s), 144.4 (s), 147.2 (s), 154.6 (s), 171.2 (s), 171.8 (s), 173.2 (s) ppm.

Anal. Calcd for $C_{40}H_{42}N_4O_6 \cdot ½\ CH_3OH$ (690.80): C, 70.42; H, 6.42; N, 8.11.
Found: C, 70.60; H, 5.99; N, 8.24.

1,4-Phenyldimethylene-bis- {2- [5-(1,5-dideoxy-3,4-dimethyl-5-oxo-2*H*-pyrrole-2-ylidene methyl)-4-methyl-2*H*-pyrrole-3-propanoic Acid Methyl Ester]} (9). Methyl 3-nor-neoxanthobilirubinate (**10**) (100 mg, 0.347 mmoles) and terephthaldicarboxaldehyde (22 mg, 0.15 mmoles) were condensed as above for **7** to afford **9** in 97% yield (98 mg) as a red-brown solid. The compound was further purified by flash chromatography (TLC on silica gel deactivated with 10% water) using dichloromethane/methanol 99:1 eluent. It had mp 290-295°C; UV-vis in Table 6; IR (KBr) ν: 3287, 2962, 1739, 1702, 1629, 1608, 1438, 1367, 1278, 1197, 1174, 1016, 819 cm^{-1}; ^{1}H-NMR ($CDCl_3$) δ: 1.95 (s, 6H), 2.10 (s, 12H), 2.56 (t, 4H, J=7.0 Hz), 2.93 (t, 4H, J=7.0 Hz), 3.70 (s, 6H), 5.87 (s, 2H), 6.89 (s, 2H), 8.21 (s, 4H), 10.4 (bs, 2H) ppm; ^{13}C-NMR ($CDCl_3$) δ: 8.69 (q), 9.63 (q), 9.82 (s), 20.02 (t), 35.26 (t), 51.76 (d), 95.16 (d), 128.1 (d), 131.0 (s), 132.6 (d), 135.0 (s), 137.1 (s), 140.2 (s), 144.1 (s), 147.4 (s), 154.9 (s), 171.1 (s), 172.2 (s), 172.8 (s) ppm.

Anal. Calcd for $C_{40}H_{42}N_4O_6$ (674.80): C, 71.20; H, 6.27; N, 8.30.
Found: C, 71.42; H, 6.14; N, 8.43.

(4Z,20Z)-2,3,7,12,13,8,22,23-Octamethyl-(1*H*,10*H*,15*H*,24*H*,25*H*,26*H*,27*H*,28*H*,29*H*)-pentapyrrin-1,24-dione-8,17-dipropanoic Acid Dimethyl Ester (4). Pentapyrrole verdin **7** (40 mg, 0.058 mmoles) was dissolved in hot tetrahydrofuran (20 mL) in a 125 mL Erlenmeyer flask and placed in a sonicator bath under a nitrogen blanket. Methanol (10 mL) was added, followed by sodium borohydride (10 mg), and the reaction was sonicated for 2 hours. Additional sodium borohydride (10 mg) was added, and the reaction was sonicated for another 3 hours. Sonication was stopped and hydrochloric acid was added until the yellow mixture's pH was 3. The mixture was taken up in dichloromethane (50 mL) and washed with water (3 x 50 mL). The organic solution was dried over sodium sulfate and filtered, and the dichloromethane was removed (roto-vap). The yellow product (**4**) was purified by flash chromatography (TLC on silica gel deactivated with 10% water) using dichloromethane/methanol 99:1 eluent. This procedure yielded 40 mg (99%) of pure product. It had mp 270-271°C; UV-vis: λ^{max} 385, ε 81,910 ($CDCl_3$), λ^{max} 383, ε 68,600 (CH_3OH), λ^{max} 409; ε 64,450 ($(CH_3)_2SO$); IR (KBr) ν: 3354, 2918, 1736, 1663, 1637, 1438, 1256, 1177, 691 cm^{-1}; ^{1}H-NMR ($CDCl_3$) δ: 1.02 (s, 6H), 1.89 (s, 6H), 2.03 (s, 6H), 2.06 (s, 6H), 2.1-2.3 (m, 4H), 2.6-2.8 (m, 4H), 3.69 (s, 3H), 3.77 (d, 2H, J=16 Hz), 3.90 (d, 2H, J=16 Hz), 5.80 (s, 2H), 8.81 (s, 1H), 10.40 (s, 2H), 10.96 (s, 2H) ppm; ^{13}C-NMR ($CDCl_3$) δ: 7.74 (q), 9.15 (q), 9.32 (q), 9.59 (q), 19.66 (t), 22.52 (t), 34.53 (t), 51.25 (d), 99.58 (d), 112.0 (s), 118.3 (s), 121.9 (s), 123.4 (s), 123.7 (s), 128.2 (s), 134.0 (s), 141.3 (s), 173.8 (s), 173.7 (s) ppm. The ester was used directly in the next step.

1,3-Phenyldimethyl-bis-{2-[5-didehydro-3,4-dimethyl-5-oxo-2*H*-pyrrole-2-ylidenemethyl)-4-methyl-1*H*-pyrrole-3-propanoic Acid Dimethyl Ester]} (5). *m*-Xylyl "verdin" **8** (90 mg, 0.134 mmoles) was dissolved in hot tetrahydrofuran (20 mL) in a 125 mL Erlenmeyer flask and placed into a sonicator under nitrogen.

Methanol (10 mL) was added, followed by sodium borohydride (10 mg) and the reaction was sonicated for 1 hour. Additional sodium borohydride (10 mg) was added and the reaction was sonicated for another hour. Sonication was stopped and hydrochloric acid was added until the yellow mixture's pH was 3. The mixture was taken up in dichloromethane (50 mL) and washed with water (3 x 50 mL). The organic solution was dried over sodium sulfate, filtered, and the dichloromethane removed (roto-vap) to give the yellow *m*-xylyl rubin ester (**5**). It was purified by flash chromatography (TLC on silica gel deactivated with 10% water) using dichloromethane/methanol 99:1 eluent to afford 85 mg (94%) of pure product. It had mp 322-325°C; UV-vis: λ^{max} 277, ϵ 16,350, λ^{max} 381, ϵ 84,810 ($CHCl_3$), λ^{max} 275, ϵ 10,000, λ^{max} 403, ϵ 58,620 (CH_3OH), λ^{max} 276, ϵ 11,010, λ^{max} 405, ϵ 61,940 ($(CH_3)_2SO$); IR (KBr) ν: 3344, 3191, 2916, 1736, 1664, 1638, 1437, 1367, 1268, 1177, 940, 691 cm^{-1}; ^{1}H-NMR ($CDCl_3$) δ: 1.02 (s, 6H), 1.76 (dt, 2H, J=8.2, 16.0 Hz), 1.92 (s, 6H), 2.07 (s, 6H), 2.15 (dt, 2H, J=8.2, 16 Hz), 2.66 (t, 4H, J=8.2), 3.67 (s, 6H), 3.80 (d, 2H, J=14.5 Hz), 4.25 (d, 2H, J=14.5), 5.80 (s, 2H), 7.19 (s, 3H), 7.80 (s, 1H), 10.72 (bs, 2H), 11.35 (bs, 3H) ppm; ^{13}C-NMR ($CDCl_3$) δ: 7.01 (q), 9.07 (q), 9.62 (q), 19.66 (t), 32.93 (t), 34.39 (t), 51.23 (d), 98.99 (d), 118.60 (s), 121.91 (s), 123.18 (s), 123.60 (s), 126.22 (d), 127.88 (d), 128.35 (s), 130.91 (d), 133.86 (s), 139.77 (s), 140.84 (s), 173.30 (s), 173.56 (s) ppm. The ester was rused directly in the next step.

1,4-Phenyldimethyl-bis- {2- [5-(1,5-dideoxy-3,4-dimethyl-5-oxo-2*H*-pyrrole-2-ylidene methyl)-4-methyl-1*H*-pyrrole-3-propanoic Acid Dimethyl Ester]} (6). *p*-Xylyl "verdin" **9** was reduced with sodium borohydride exactly as for **5** above to give 85 mg (94%) of desired product (**6**). It had mp 382-390°C; UV-vis: λ^{max} 280, λ^{max} 408 ($CHCl_3$); λ^{max} 280, λ^{max} 410 (CH_3OH); λ^{max} 2783, λ^{max} 408 ($(CH_3)_2SO$); IR (KBr) ν: 3340, 3154, 2917, 1736, 1664, 1635, 1459, 1263, 1177, 692 cm^{-1}; ^{1}H-NMR ($(CD_3)_2SO$) δ: 1.72 (s, 6H), 1.98 (s, 6H), 2.01 (s, 6H), 2.20 (t, 4H, J=7.0 Hz), 2.52 (t, 4H, J=7.0), 3.49 (s, 6H), 3.83 (s, 4H), 5.88 (s, 2H), 7.03 (s, 4H), 9.75 (bs, 2H), 10.33 (bs, 2H) ppm; ^{13}C-NMR: not soluble in $CDCl_3$ or $(CD_3)_2SO$. The ester was used directly in the next step.

(4Z,20Z)-2,3,7,12,13,18,22,23-Octamethyl- (1*H*,10*H*,15*H*,24*H*,25*H*,26*H*,27*H*,28*H*,29*H*)-pentapyrrin-1, 24-dione-8,17-dipropanoic Acid (1). In a 100 mL round-bottom flask equipped for heating mantle and reflux, dimethyl ester **4** (40 mg, 0.058 mmoles) was dissolved in tetrahydrofuran (20 mL) with methanol (20 mL). Sodium hydroxide (1 mL of 1 M) was added, and the solution was heated at reflux for 3 hours under nitrogen and in the dark. The solution was cooled, and the solvents were removed (roto-vap). Water (20 mL) was added to redissolve the salts, and the solution was acidified to pH 5 with 1 *M* hydrochloric acid. The resulting precipitate was allowed to stir in the acid solution for 20 minutes and then was collected by centrifugation. The yellow pentapyrrole rubin was washed with water (2 x 20 mL), re-centrifuging each time, and then collected by filtration. This procedure yielded 32 mg (82%) of the desired product. It had mp >350° (d); UV-vis in Table 3; IR (KBr) ν: 3353, 3154, 2923, 1662, 1637, 1400, 1266, 1177, 940, 690 cm^{-1}; ^{1}H-NMR in Table 2; ^{13}C-NMR in Table 1.

Anal. Calcd for $C_{38}H_{45}N_5O_6$ (667): C, 68.35; H, 6.79; N, 10.49.
Found: C, 68.09; H, 6.69; N, 10.32.

1,3-Phenyldimethyl-bis- {2-[5-(1,5-dideoxy-3,4-dimethyl-5-oxo-2*H*-pyrrole-2-ylidene methyl)-4-methyl-1*H*-pyrrole-3-propanoic Acid]} (2). Expanded rubin ester **5** was saponified exactly as for **4** to give 70.1

mg (86%) of the desired product **2**. It had mp 285-290°C; IR (KBr) ν: 3347, 3142, 2919, 1664, 1638, 1458, 1400, 1269, 1178, 941, 691 cm^{-1}; UV-vis in Table 3; ^{1}H-NMR in Table 2; ^{13}C-NMR in Table 1.

Anal. Calcd for $C_{38}H_{42}N_4O_6$ (650.8): C, 70.13; H, 6.51; N, 8.61.
Found: C, 69.82; H, 6.20; N, 8.49.

1,4-Phenyldimethyl-bis- {2-[5-(1,5-dideoxy-3,4-dimethyl-5-oxo-2*H*-pyrrole-2-ylidene methyl)-4-methyl-1*H*-pyrrole-3-propanoic Acid]} (3). Expanded rubin ester **6** (85 mg, 0.125 mmoles) was suspended in ethanol (50 mL), sodium hydroxide (1 mL, 1 *M*) was added, and the solution was heated at reflux for 18 hours under nitrogen and in the dark. The solution was cooled, and the ethanol was removed (roto-vap). Water (20 mL) was added to redissolve the salts, and the solution was acidified to pH 5 with 1 *M* hydrochloric acid. The resulting precipitate was allowed to stir in the acid solution for 20 minutes and was collected by centrifugation. The yellow product (**3**) was washed with water (2 x 20 mL) re-centrifuging each time, then collected by filtration to afford 76.3 mg (94%) of pure rubin **3**. It had mp >400°C d; IR (KBr) ν: 3350, 3142, 2907, 1654, 1642, 1400, 1177 cm^{-1}; UV-vis in Table 3; ^{1}H-NMR in Table 2; ^{13}C-NMR in Table 1.

Anal. Calcd for $C_{38}H_{42}N_4O_6$ (650): C, 70.13; H, 6.51; N, 8.61.
Found: C, 69.73; H, 6.21; N, 7.81.
Anal. HRMS (FAB) Calcd for $C_{38}N_{43}O_6$ $[M+H]^+$: 651.3183. Found: 651.3154.

Molecular Dynamics. Molecular mechanics calculations and molecular modelling was carried out as described previously[5] on an Evans and Sutherland ESV-10 workstation using version 5.41 of SYBYL (Tripos Assoc., St. Louis, MO). The conformational energy maps were created using Wingz™ (Informix), and the ball and stick drawings were created from the atomic coordinates of the molecular dynamics structures using Müller and Falk's "Ball and Stick" program (Cherwell Scientific, Oxford, U.K.) for the Macintosh.

Acknowledgements: We thank the National Institutes of Health (HD17779) for generous support.

REFERENCES

1. Maisels, M.J. *Clinics in perinatology. Neonatal Jaundice.* **1990**, Saunders, W.B., Philadelphia, Vol. 17, No. 2.

2. McDonagh, A.F. in *The Porphyrins*; Dolphin, D., ed.; Academic Press: New York, **1979**; Vol. 6, pp 293-491.

3. For leading references see Lightner, D.A.; McDonagh, A.F. *Acc. Chem. Res.*, **1984**, *17*, 417-424.

4. For leading references see Falk, H. *The Chemistry of Linear Oligopyrroles and Bile Pigments*, Springer Verlag: New York, 1989.

5. Person, R.V.; Peterson, B.R.; Lightner, D.A. *J. Am. Chem. Soc.*, **1994**, *116*, 42-59.

6. Boiadjiev, S.; Person, R.V.; Puzicha, G.; Knobler, C.; Trueblood, K.N.; Lightner, D.A. *J. Am. Chem. Soc.*, **1992**, *114*, 10123-10133.

7. (a) Bonnett, R.; Davies, J.E.; Hursthouse, M.B.; Sheldrick, G.M. *Proc. R. Soc. Chem.* **1978**, *B202*, 249-268.

(b) LeBas, G.; Allegret, A.; Mauguen, Y.; Derango, C; Bailly, M. *Acta Crystallogr.* **1980**, *B36*, 3007-3011.

8. (a) Kaplan, D.; Navon, G. *Isr. J. Chem.* **1983**, *23*, 177-186.
(b) Kaplan, D.; Navon, G. *Biochem. J.* **1982**, *201*, 605-613.
(c) Navon, G; Frank, S.; Kaplan, D. *J.C.S. Perkin Trans. 2* **1984**, 1145-1149.

9. Yang, B; Morris, M.D.; Xie, M; Lightner, D.A. *Biochemistry, 30*, **1991**, 688-694.

10. Zakim, D; Wong, P.T.T. *Biochemistry, 29* **1990**, 2003-2007.

11. Lightner, D.A.; Wijekoon, W.M.D.; Zhang, M-H. *J. Biol. Chem.* **1988**, *263*, 16669-16676.

12. (a) Lauffer, R.B.; Vincent, A.C.; Padmanabhan, S.; Meade, T.J. *J. Am. Chem. Soc. 109*, **1987**, 2216-2219.
(b) Hsieh, H.S.; Morris, M.D. *J. Am. Chem. Soc., 110*, **1988**, 62-67.

13. Hahm, J-S.; Ostrow, J.D.; Mukerjee, P., Celic, L. *J. Lipid Res., 33*, **1992**, 1123-1137.

14. Pu, Y.M.; Lightner, D.A. *Tetrahedron, 47*, **1991**, 6163-6170.

15. Mugnoli, A.; Manitto, P.; Monti, D. *Acta Crystallogr.* **1983**, *C38*, 1287-1291.

16. McDonagh, A.F.; Lightner, D.A. In *Hepatic Metabolism and Disposition of Endo and Xenobiotics*, Kluwer, Dordrecht, The Netherlands, **1991**, Chap. 5, 47-59.

17. Ostrow, J.D., ed. *Bile Pigments and Jaundice*; Marcel Dekker: New York, 1986.

18. Trull, F.R.; Franklin, R.W.; Lightner, D.A. *J. Heterocyclic Chem.*, **1987**, *24*, 1573-1579.

19. Hwang, K.H.; Lightner, D.A. *Heterocycles*, **1994**, in press.

20. Xie, M.; Lightner, D.A. *Tetrahedron*, **1993**, *49*, 2185-2200.

21. (a) Falk, H.; Flödl, H. *Monatsh.*, **1985**, *116*, 1177-1187.
(b) Falk, H.; Flödl, H. *Monatsh.*, **1986**, *117*, 57-67.

22. Woodward, R.B.; Ayer, W.A.; Beaton, J.M.; Bickelhaupt, F.; Bonnett, R.; Buchschacher, P.; Closs, G.L.; Dutler, H.; Hannah, J.; Hauck, F.P.; Itô, S.; Langemann, A.; LeGoff, E.; Leimgruber, W.; Lwówski, W.; Sauer, J.; Valenta, Z.; Volz, H. *Tetrahedron*, **1990**, *46*, issue No. 27.

23. Fischer, H.; Hofelmann, H. *Ann. Chem.*, **1938**, *533*, 216-230.

24. Silverstein, R.M.; Ryskiewicz, D.D.; Willand, C. *Org. Synth.*, **1963**, Coll. Vol. IV, 831-833.

25. Trull, F.R.; Ma, J.S.; Landen, G.L.; Lightner, D.A. *Israel J. Chem.*, **1983**, *23 (2)*, 211-218.

26. McDonagh, A.F.; Palma, L.A.; Trull, F.R.; Lightner, D.A. *J. Am. Chem. Soc.*, **1982**, *104*, 6865-6867.

27. Kasha, M.; Rawls, H.R.; El-Bayoumi, M.A. *Pure Appl. Chem.*, **1965**, *32*, 371-392.

(*Received in USA* 22 *March* 1994; *accepted* 20 *May* 1994)